FLYBUSRI

Middle East Technical University

Department of Electrical and Electronics Engineering

EE464: Static Power Conversion II

Term Project Final Report

Group Name: FlyBusri

Student 1: Elif Topaloğlu - 2443984

Student 2: Caner Aydın - 2374528

Student 3: Doruk Yazıcı - 2517225

Submission Date: 14.06.2024

Table of Contents

Introduction

The aim of the project is to design and implement an “Isolated DC-DC Battery Charger”, whose specs will be given in the upcoming parts of the report. In this report, design decisions will be investigated, the transformer design for the selected topology will be explained, the circuit manufactured according to the simulations done will be clarified, closed-loop control loop of the design will be made clear, and the real-life test results will be presented.

All of the documents, simulations and sources related to the design of the converter is published in the “GitHub Repository” of the project.

The project is completed, but it is still open for improvements.

Project Definition

An isolated DC-DC converter will be designed in whose topology can be selected in a way which suits the groups. The specs of the project are:

- **Minimum Input Voltage:** $20V$
- **Maximum Input Voltage:** $40V$
- **Output Voltage:** $12V$
- **Output Power:** $60W$
- **Output Voltage Peak-to-Peak Ripple**: 3%
- **Line Regulation:** 3%
- **Load Regulation:** 3%
- **Closed-Loop Control** is a must.

Topology Selection

To control the output current and voltage while achieving high efficiency in this project, a proper isolated DC-DC converter topology should be selected. In this section, several isolated converter topologies are considered and compared to select the most suitable one.

- **Flyback Converter*:*** This topology is one of the simplest designs that can be used in order to design an isolated DC-DC converter. It is advantageous due to uncomplicated design procedure since it only utilizes a single active switch. Moreover, a lower number of components are needed compared to the other types of topologies for this converter. A lower number of components makes sure that the design is cost effective compared to the other types of topologies which is an important advantage of this topology. Also,

flyback converter is generally a good choice for low power applications which is smaller than 200W as it is the case for this project.

Apart from several handy advantages, there are multiple disadvantages of this topology as it single-ended type converter which means that it operates at a single quadrant of the BH curve. Also, it charges and discharges the inductors at different switching cycles, a gapped core is essential to increase the energy storage capacity. Thus, the main disadvantage can be poor transformer utilization. Moreover, due to high ripple currents at the input and output sides stemming from low inductance of the gapped core, larger capacitors should be utilized which is also a disadvantage for this topology.

- **Forward Converter*:*** This converter is mainly used for medium power applications in practice. One of the best advantages compared to the flyback is that the energy does not need to be stored as it is transferred in at the same cycle that is created. Thus, the magnetic core can be gapless, and the transformer utilization is better [2]. Using a gapless converter reduces the current ripple; thus, efficiency can be increased, and smaller rating components can be used which will probably lead to more compact design compared to the flyback converter.

  The drawbacks compared to the flyback converter can be the increased cost as it uses an extra diode and an inductor, which is an important issue for low-budget projects. Moreover, as the energy is transferred for the same cycle, magnetizing current should be reset before the nest switching cycle which limits the maximum duty to 50%. If the transformer is not properly designed and controlled, higher duty cycle than 50% will lead to saturation of the core which makes a sensitive control system a must for this topology. Also, in the practical design, a third winding is added to protect the circuit from the leakage inductance effects. However, due to this winding, voltage across the primary switch is increased which results in higher voltage stress across the switch which is an important disadvantage which needs to be handled.

- **Push-Pull Converter:** The main application area consists of higher power applications since the power is distributed and handled by two active switches. Also, this topology differs from the previous two as it is double-sided which implies that the transformer is operating at two quadrants of the magnetic core which results in better utilization of the transformer. Therefore, this is a good choice for high power applications due to high efficiency.

  However, due to the increased number of active switches, the total cost of this topology is fairly high compared to the other two. Also, control of these two active switches is more complex since the dead time should be arranged properly in order not to short circuit the source at the input. Moreover, a center-tapped transformer is used in this topology; thus, overall, the design procedure, when two active switches and

transformer design is considered, is more complex. Finally, when two switches are off, voltage stress across the two switches is still quite high, which may cause problems when the switch is not properly selected and cause heating problems as well as increased losses due to possible high on resistances.

- **Half-Bridge and Full-Bridge Converters:** These two topologies are also used for high power applications, generally higher than push-pull converters. The advantage of these two compared to the push-pull converter is that the voltage stress across the switches is decreased. Moreover, these are also double sided; however, they have single primary winding which makes sure that the transformer is utilized better compared to the push-pull converter [2].

  The disadvantage of these topologies is that half-bridge cost is slightly more than the push-pull converter. For the full-bridge converter, the cost is considerably higher as it includes 4 active switches which also complexes the design and the controllers. These topologies become an overdesign for low power applications.

  Considering all of the mentioned topologies, and the low output power requirement of the project, push-pull, half-bridge and low-bridge converters are found to be overcomplicated for this specific application. Also, as the cost and complexity are important points for this project, flyback converter topology is found to be applicable and sufficient. In the nest section, a flyback converter will be designed and presented.

Validation of Design

General Design

For this project, as explained in the previous section, a flyback converter has been selected. The general topology schematic is given below. In order to avoid sudden current changes due to the leakage inductance, and the additional losses occuring due to the ringint of voltage on the MOSFET switch and secondary side diode, an RCD snubber design is added to ensure the safety of the design and the switch.

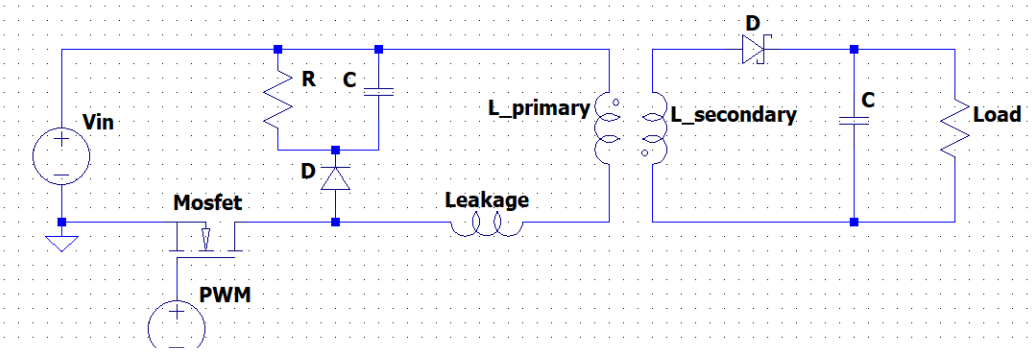

Figure 1. Flyback Converter Topology

As a closed-loop control is mandatory for the project, a controller needs to be used to ensure that the voltage at the output is 12V continuously. For this reason, an analog controller will be utilized. Due to the low side placement of the MOSFET, driver circuitry will be simpler and there will be no need for a bootstrap circuit, only a MOSFET gate driver integrated circuit will be utilized, as the output current of the analog controller may not be able to operate open the gate of the MOSFET. To ensure the isolation boundary is preserved, an optocoupler is used for the closed loop control. In the following section, analytical calculations for the transformer design and RCD snubber design will be presented.

Transformer Design

To start with the magnetic design of the topology, duty cycle should be decided to calculate the corresponding turns ratio. In flyback converters, duty cycle can obtain values between zero and one. However large duty cycle values do not assure a good performance. If the input voltage is low, which implies a high duty cycle, conduction losses will increase due to increased conduction time. Moreover, for a poorly designed transformer, large duty values may result in core saturation due to decreased allocation time for the flux reduction inside the core. Both situations decrease the efficiency of the converter which is unwanted. Thus, maximum duty cycle is selected as 0.5 for this design. When the maximum duty cycle is selected, maximum turns ratio can be calculated using the following formula below. The important point in this calculation is that output voltage is taken as 13V to consider the voltage drop across the output diode and to stay within the predefined duty cycle limits. For ease of manufacturing and simplicity, turns ratio is selected as 1. For the selected turns ratio, duty cycle for both input voltages is calculated below.

$$\frac{N_1}{N_2} \leq \frac{Vin * D}{(Vout + 1) * (1 - D)}$$

$$\frac{N_1}{N_2} \leq \frac{20 * 0.5}{13 * (1 - 0.5)} \cong 1.54\ turns$$

$$D = \frac{1}{\left(\frac{V_{in}}{V_{out} + 1} + 1\right)}$$

$$D_{max} = \frac{1}{(\frac{20}{13} + 1)} = 0.393 \cong 0.4 \ \ \& \ \ D_{min} = \frac{1}{\left(\frac{40}{13} + 1\right)} = 0.245$$

Table 1. Turns Ratio Selection and Duty Cycle Limits

Turns Ratio (N1/N2)	1
Duty Cycle Range	0 to 0.5
Maximum Duty Cycle	0.393
Minimum Duty Cycle	0.245

At this point, a target efficiency should be selected in order to move on to further parameter calculation. Target efficiency is selected as:

$$\eta_{target} = 0.8$$

After determining the efficiency target, input power can be calculated:

$$P_{in} = \frac{P_{out}}{\eta_{target}} = \frac{60W}{0.8} = 75W$$

Knowing the limits of the duty cycles, the average current flowing on the magnetizing inductance during on period when the input voltage is in its low limit can be calculated as [3]:

$$I_{EDC} = \frac{P_{in}}{V_{in,min} \cdot D_{max}} = \frac{75W}{20V \cdot 0.4} = 9.375A$$

At this point, another design decision should be given which is the value for K_{RF}, which denotes "current ripple factor". Here, the current ripple factor is selected as $K_{RF} = 0.33$ which is within the reasonable limit as stated in the design document. Thus, the current ripple is calculated as below.

$$\Delta I = 2 \cdot K_{RF} \cdot I_{EDC} = 2 \cdot 0.33 \cdot 9.375 = 6.1875A$$

Then:

$$I_{EDC,max} = 9.375 + \frac{6.1875}{2} = 12.47A \cong 12.5A$$
$$I_{EDC,min} = 9.375 - \frac{6.1875}{2} = 6.28A \cong 6.3A$$

This shows that the peak current on the inductor and hence the MOSFET is approximately $12.5A$.

As the minimum primary inductor voltage, the switching frequency, the duty cycle at the minimum voltage and current ripple are known, the inductance of the primary inductor can be easily calculated using the inductor equation:

$$V_L = L \cdot \frac{di}{dt}$$

Considering the on period, the same equation can be converted to the equation below. Assuming a higher current ripple factor for the higher value of the input voltage, the same equation can be written as:

$$V_L = L \cdot \frac{\Delta i}{D \cdot T_s} \rightarrow L_{min} = \frac{V_L \cdot D \cdot T_s}{\Delta i} = \frac{V_{in,max} \cdot D_{min}}{f_{sw} \cdot \Delta i} = \frac{40V \cdot 0.245}{100kHz \cdot 6.1875A} = 19.79\mu H$$

Leaving a safety margin which will in fact lower the voltage ripples on the magnetizing inductance, the primary inductance of the transformer is selected as:

$$L_m = 20\mu H$$

At this point, the core material is decided. In order to increase the energy storage capacity for the flyback converter, the core should have an airgap. After some research, the core found is "B66363G0500X187" which is an N87 type ETD39 ferrite core from TDK Electronics. It has a built-in 0.5mm airgap so that when two of them are used, a total of 1mm airgap will be obtained. Datasheet of the core provides some valuable information considering the airgaps:

$$A_L = \frac{196nH}{T^2} \;\&\; \mu_r = 115 \;\&\; I_e = 92.2mm$$

To find the number of turns in the primary side:

$$20\mu H = \frac{196nH}{T^2} \cdot N^2 \rightarrow N = 10.1\, Turns$$

The turn number is required as an integer and considering the safety left at the inductance value, the turn number selection is made as:

$$N = 11\, Turns \rightarrow L_m = 23.71\mu H$$

As the turns ratio is selected as 1, the secondary side will have the same number of turns.

Then, to find the magnetic flux density (B) inside the core, the magnetic field intensity is found using Ampere's Circuital Law:

$$N \cdot I_{max} = H_{max} \cdot \int dL \rightarrow 11 \cdot 12.5A = H_{max} \cdot 92 \cdot 10^{-3}m$$

$$H_{max} = 1490.50\frac{A}{m}$$

Then:

$$B_{max} = \mu_0 \cdot \mu_r \cdot H_{max} = 4\pi \cdot 10^{-7} \cdot 115 \cdot 1355.75\frac{A}{m} = 0.215T$$

Considering the information given in the datasheet of N87 materials by TDK Electronics, the found value is far away from the saturation of the core, which is given approximately as $0.4T$.

Considering the operating frequency of $80kHz$, the cable is selected as "AWG26" since it offers an operating frequency of $107kHz$ for maximum skin depth. To be able to calculate the number of parallelled conductors, the RMS value of the current flowing through the transformer should be found. RMS value for a triangular wave with an offset can be calculated using the formula given below [4].

$$I_{RMS} = I_{EDC} * \sqrt{1 + \frac{1}{12} * \left(\frac{\Delta I}{I_{EDC}}\right)^2}$$

$$I_{RMS} = 9.375 * \sqrt{1 + \frac{1}{12} * \left(\frac{6.1875}{9.375}\right)^2} \cong 9.54A$$

The AWG26 cable can carry $0.361 \frac{A}{conductor}$ so that the number of conductors that should be wound together is as follows.

$$\frac{9.54}{0.361} \cong 26.44 \rightarrow 27 \; will \; be \; used$$

One AWG26 cable has a conductor cross section of $0.128\ mm^2$ but considering the isolation on them, this value will be taken as $0.14\ mm^2$ for more realistic calculations. Assuming same number of conductors will be used for both the primary and secondary sides, the total area that will be occupied by the conductors can be calculated as:

$$2 \cdot 0.14mm^2 \cdot 27 \cdot 10 = 75.6\ mm^2$$

TDK Electronics recommends coil formers B66364B1016T001 or B66364W1016T001 to be used with the selected core which offer $178mm^2$ of window area.

This results in a fill factor of:

$$Fill\ Factor = \frac{75.6\ mm^2}{178\ mm^2} \cong 0.42$$

which is a reasonable value.

In the table of AWG cables, the resistance of the AWG26 cable is given as $\frac{133.8568\Omega}{1000m}$. The mean path length of the coil formers is given as $69mm$. For the primary or the secondary side, the total DC resistance can be calculated as:

$$R_{DC} = 10 \cdot 69 \cdot 10^{-3}m \cdot \frac{133.8568\Omega}{1000m} \cdot \frac{1}{20} = 4.618 \cdot 10^{-3}\Omega$$

The AC resistance can be calculated as follows:

$$R_{AC} = \frac{\rho \cdot l}{A_{eff}} \;\&\; A_{eff} = \delta \cdot \pi \cdot d \;\&\; \delta = \sqrt{\frac{\rho}{\pi \cdot f \cdot \mu}}$$

$$\delta = \sqrt{\frac{1.678 \cdot 10^{-8}}{\pi \cdot 80 \cdot 10^3 \cdot 4\pi \cdot 10^{-7} \cdot 0.999991}} = 230.5 \cdot 10^{-6}m$$

Since the skin depth is larger than the actual cross section of the cable, effective area is taken as the cable's cross section area assuming that the current will flow uniformly.

$$A_{eff} = 230.5 \cdot 10^{-6}m \cdot \pi \cdot 0.40386 \cdot 10^{-3}m = 292.45 \cdot 10^{-9}m^2$$

$$R_{AC} = \frac{1.678 \cdot 10^{-8} \cdot 10 \cdot 69 \cdot 10^{-3}}{0.128 * 10^{-6}} \cdot \frac{1}{20} = 4.52 * 10^{-3}\Omega$$

It can be seen that the AC and DC resistances of AWG26 cable at the specified frequency is almost same. It is expected that AC resistance should be higher than the DC resistance, which is not the case, and this will probably stem from the given resistance multiplier in the datasheet for the DC resistance.

The total copper loss can be calculated as:

$$P_{cu} = 2 \cdot I_{DS,RMS}^2 \cdot R_{DC} = 2 \cdot 9.54^2 \cdot 4.687 \cdot 10^{-3} = 0.85W$$

As stated before, the core material is N87. Reading the datasheet of the "N87 SIFERRIT Material", the core loss values for some frequency and Tesla values can be found. In the datasheet, the core loss for $80kHz$ and $200mT$ at $100°C$ is given approximately as $280\frac{kW}{m^3}$. The datasheet of the B66363G0500X187 core states that the volume of a core is $11500mm^3$. Then:

$$P_{core} = 280\frac{kW}{m^3} \cdot 11500 \cdot 10^{-9}mm^3 = 3.22W$$

The total loss of the transformer can be estimated as:

$$P_{loss} = P_{core} + P_{cu} = 3.22W + 0.85W = 4.07W$$

The design does not require new iterations as the values are in acceptable limits, and most importantly the cores are found in a distributor in Turkey, who can bring them with all the additional materials in 10 days maximum. For the wire, instead of wounding tons of AWG cables together, the "Litz Wire" is used which is supplied by "METU Powerlab", greetings to them (especially to Ogün Altun).

RCD Snubber Design

For the RCD snubber design, a handbook is found from Fairchild. A proper RCD snubber should be utilized in order to avoid the devastating effect of leakage inductance. Snubber values are calculated below using the formulas presented in the handbook.

$$R_{sb} = \frac{V_{sb}^2 * (V_{sb} - nV_o)}{0.5 * L_{leakage} * I_{peak}^2 * V_{sb} * f_s}$$

$$C_{sb} = \frac{V_{sb}}{R_{sn} * \Delta V_{sb} * f_s}$$

These values should be obtained using simulation software. Simulation results will be presented in the following part; however, using the values obtained from the simulation,

snubber values can be calculated using the given formulas above. The calculations are presented below.

$$R_{sb} = \frac{30^2 * (30 - 12)}{0.5 * 0.25 * 10^{-6} * 11.5^2 * 30 * 80 * 10^3} = 408\ \Omega$$

$$C_{sb} = \frac{30}{408 * 2.9 * 80 * 10^3} = 317\ nF$$

In the following section, using the analytical calculations, simulations results will be presented in order to validate the design.

Open-Loop Simulation Results

To be able to validate the various design decisions taken, an open-loop simulation is created as the first step. The simulation is run for input voltages of 20V and 40V separately, and the results will be presented separately also. The circuit schematic can be seen in Figure 2.

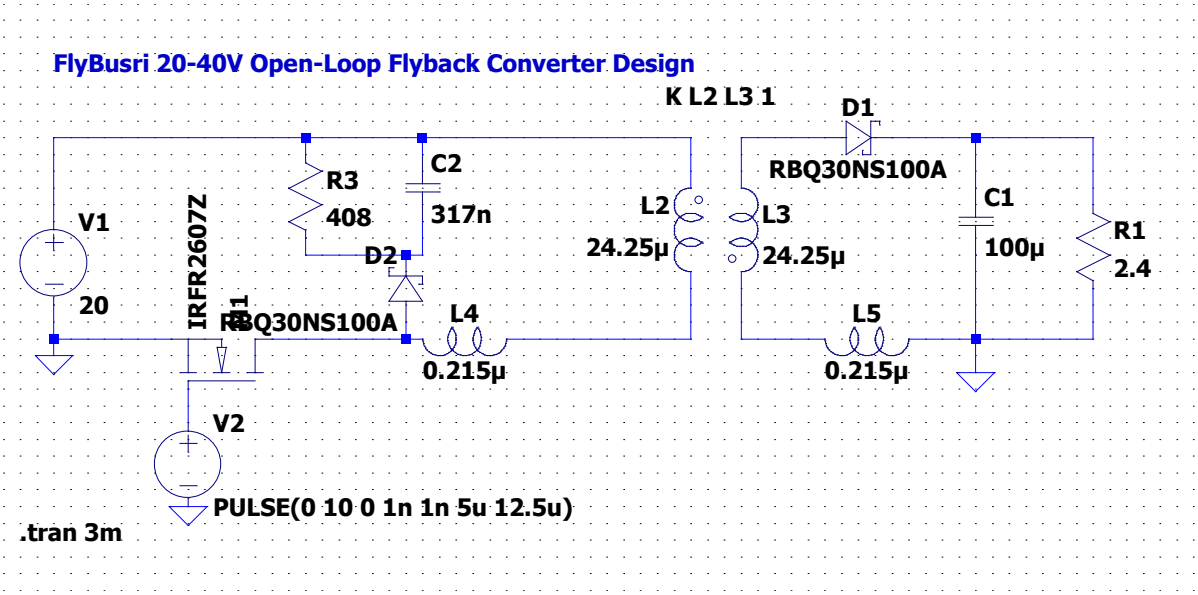

Figure 2. Circuit Schematic of the Open-Loop Flyback Converter

First of all, the input voltage is set as 20V, and the duty cycle is set as 0.4. It should be noted that all of the measurements are taken in the steady state, and with the tools of LTSpice.

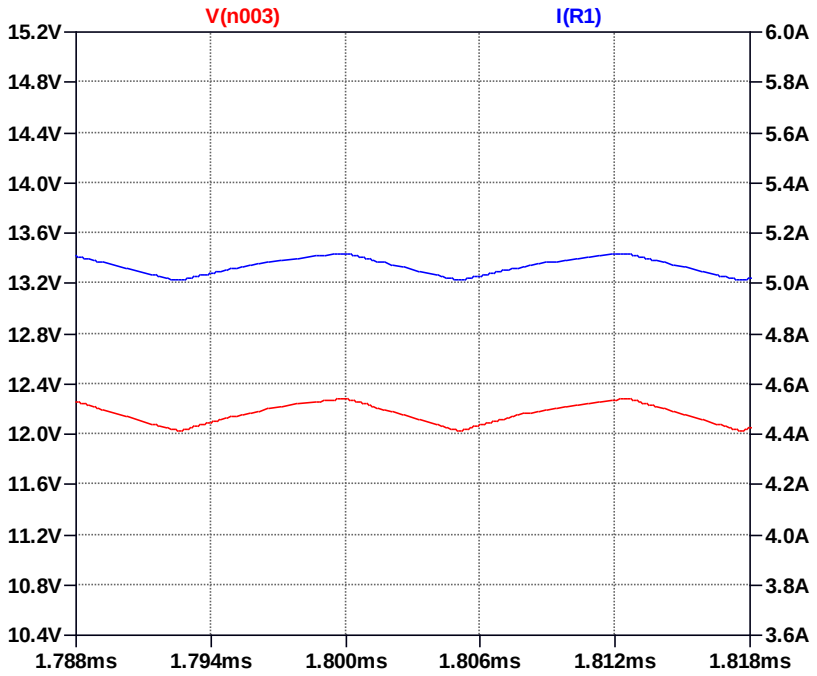

Figure 3. Output Voltage and Current Measurements for Vin = 20V

The average output voltage is measured as 12.141V, and the average output current is measured as 5.059A which results in an average output power of 61.398W. The average input power is measured as 75.738W which results in an efficiency of 0.811.

The ripple on the output voltage is equal to 249.85mV at steady state which results in an output voltage regulation of 2.06%.

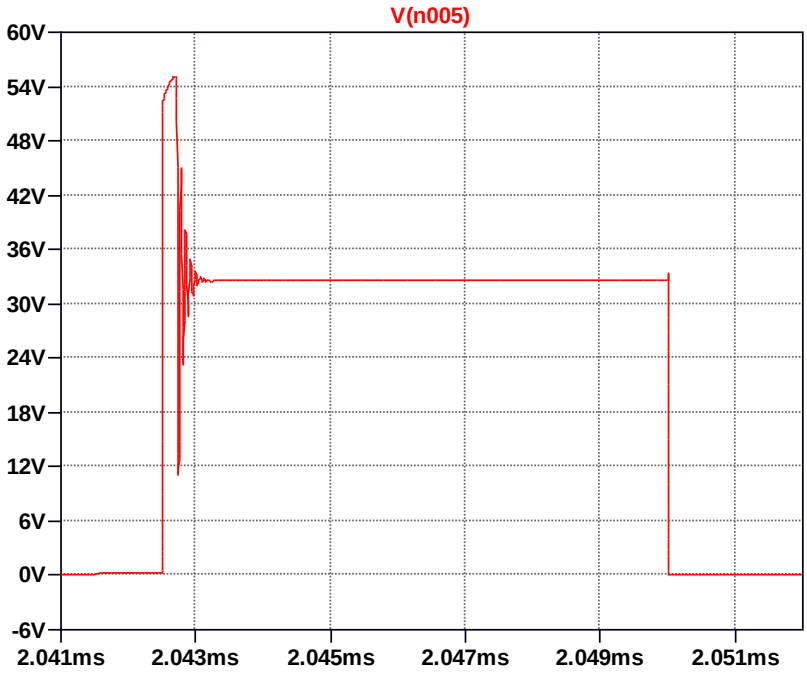

Figure 4. Vds Measurements on the MOSFET for Vin = 20V

The maximum voltage measured on the MOSFET is 55.2V at the steady state. During startup, the voltage on the MOSFET increases to 90V for an instance.

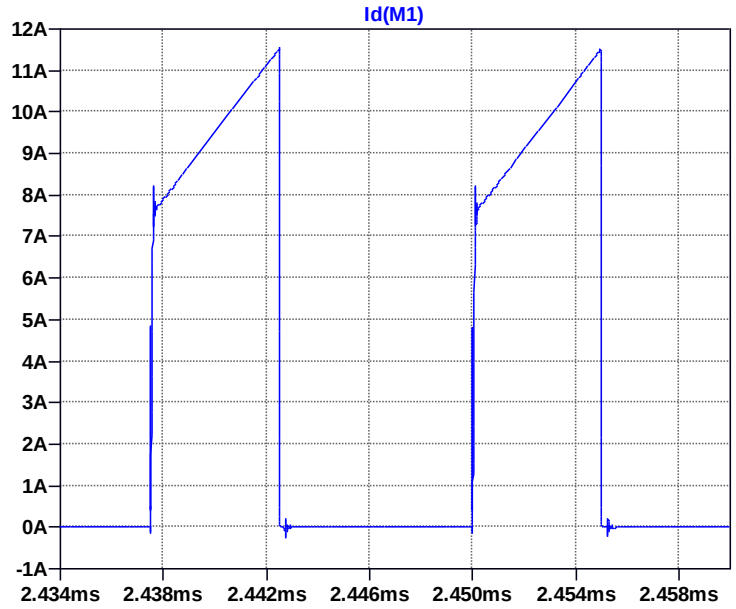

Figure 5. Ids Measurements on the MOSFET for Vin = 20V

The current on the MOSFET increases to 11.51A from 7.63A during the ON period. During startup, the current on the MOSFET increases to 27A for an instance. These maximum values of current and voltage on the MOSFET are considered when the components are chosen.

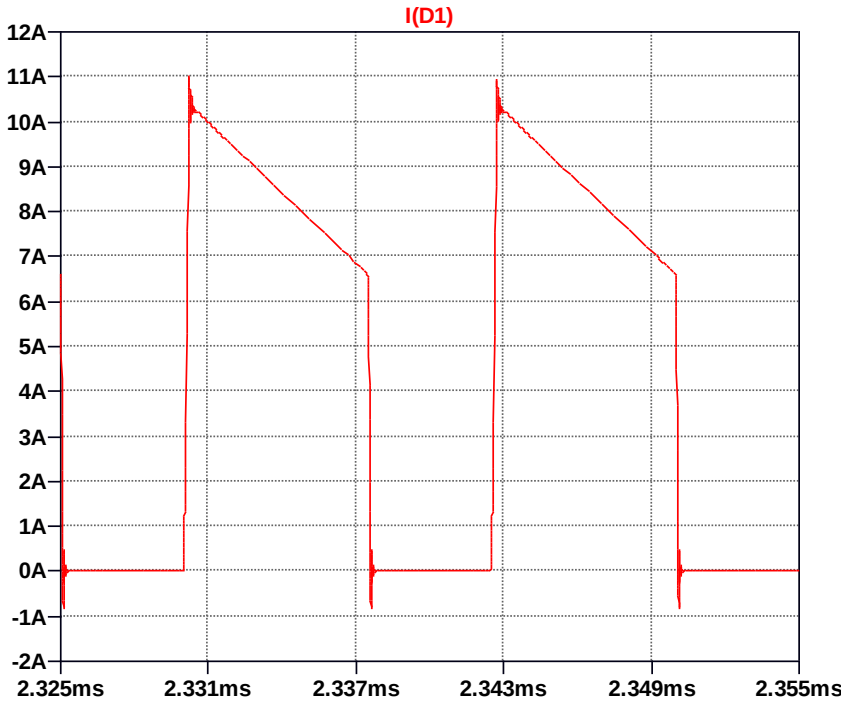

Figure 6. Forward Current on the Output Diode for Vin = 20V

The current on the output diode decreases to 6.64A from 10.95A during a cycle. During startup, the current on the output diode reaches 27A for an instance.

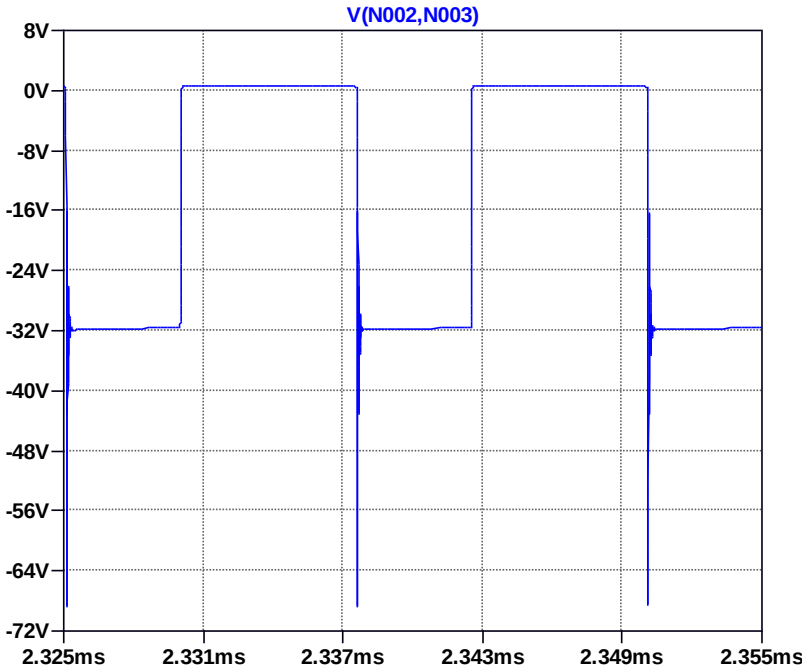

Figure 7. Voltage on the Output Diode for Vin = 20V

The output diode should be able to stand a reverse voltage of 68.54V. During startup, this value reaches up to 79V. These maximum values of current and voltage on the output diode are considered when the components are chosen.

Then, the input voltage is set to 40V and the duty cycle is set as 0.245.

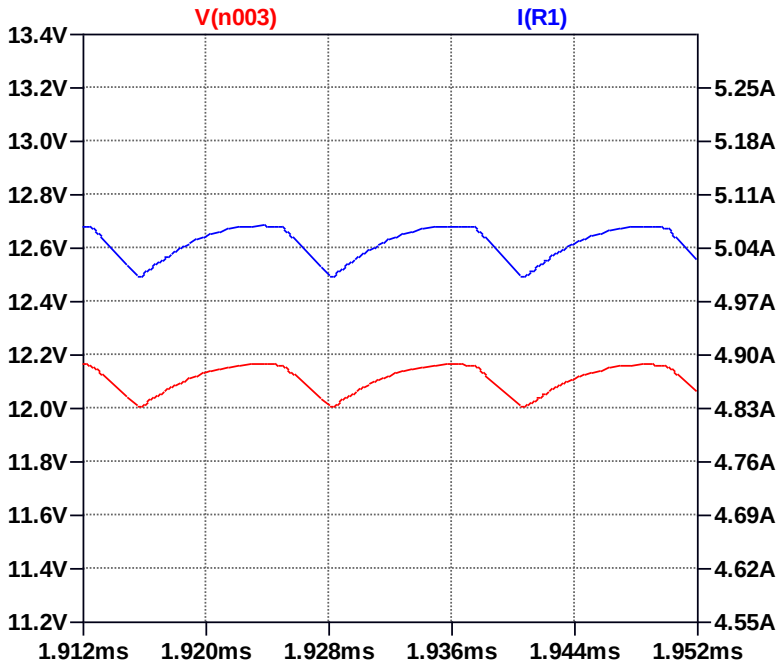

Figure 8. Output Voltage and Current Measurements for Vin = 40V

The average output voltage is measured as 12.101V, and the average output current is measured as 5.042A which results in an average output power of 60.994W. The average input power is measured as 81.95W which results in an efficiency of 0.744.

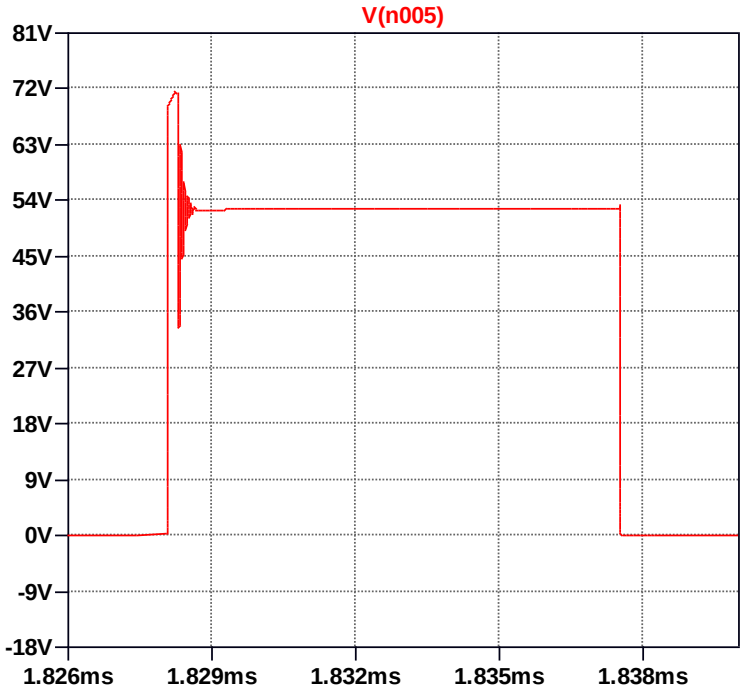

Figure 9. Vds Measurements on the MOSFET for Vin = 40V

The ripple on the output voltage is equal to 161.26mV at steady state which results in an output voltage regulation of 1.33%.

The maximum voltage measured on the MOSFET is 71.3V at the steady state. During startup, the voltage on the MOSFET increases to 107V for an instance.

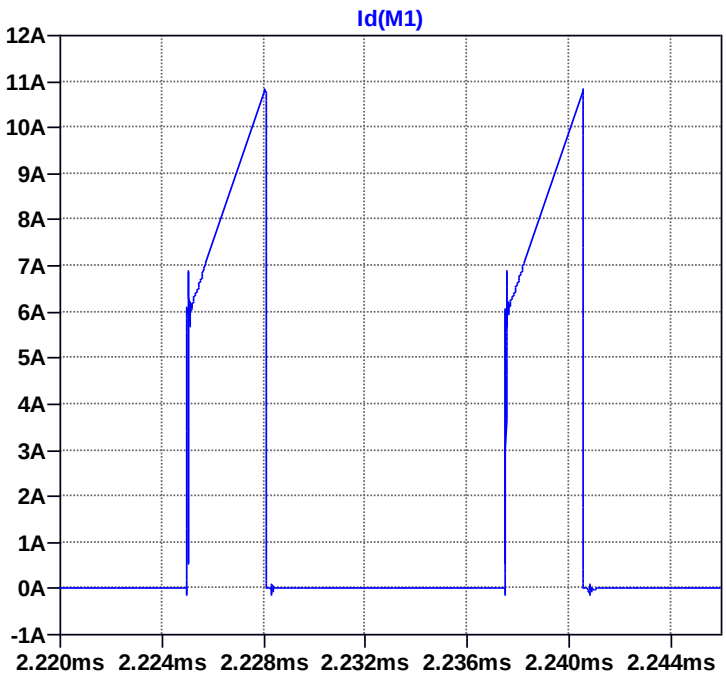

Figure 10. Ids Measurements on the MOSFET for Vin = 40V

The current on the MOSFET increases to 10.86A from 6.16A during the ON period. During startup, the current on the MOSFET increases to 27A for an instance. These maximum values of current and voltage on the MOSFET are considered when the components are chosen.

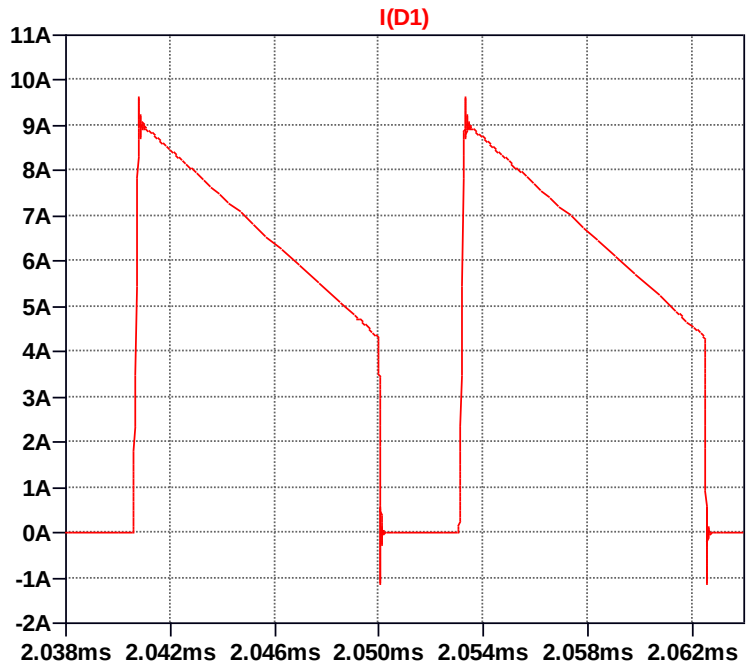

Figure 11. Forward Current on the Output Diode for Vin = 40V

The current on the output diode decreases to 4.36A from 9.32A during a cycle. During startup, the current on the output diode reaches 27A for an instance.

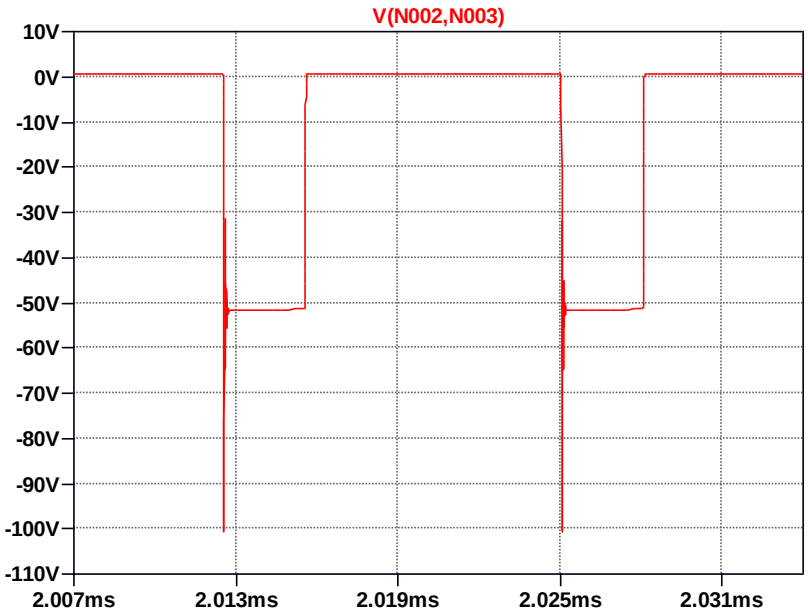

Figure 12. Voltage on the Output Diode for Vin = 40V

The output diode should be able to stand a reverse voltage of 100.59V. During startup, this value reaches up to 101V. These maximum values of current and voltage on the output diode are considered when the components are chosen.

The open-loop simulation is a good first step towards the design process, but a closed-loop simulation should be implemented for a better visualization of the real-world design.

Closed-Loop Simulation Results

For a real-world application, a closed-loop system should be designed so that the system can respond to changes in the input and regulate a better output even if the output load changes also.

It was stated that the bonus for using an analog IC is aimed so that a closed-loop design using an analog IC is generated. For the design, the “WEBENCH Power Designer” tool from the Texas Instruments. From many options generated, the one that uses UC3845 Analog IC is selected as the mentioned IC can be found easily in Turkey, and it fits the design considerations. A critical point is that the series of ICs “UC384x” are very similar in terms of properties. The only difference of UC3845 is that the maximum duty cycle it can generate at its output pin is 50%. As mentioned before, the maximum duty cycle for the application is less than 50%, so that the other ICs of the same family can be used, according to the stocks that are present in Turkey.. Another advantage of the circuit is that by changing some of the feedback resistances, the output voltage can be regulated easily, if there is a need for that. Also, the feedback loop can be updated.

The reference design obtained from the tool can be seen in Figure 13.

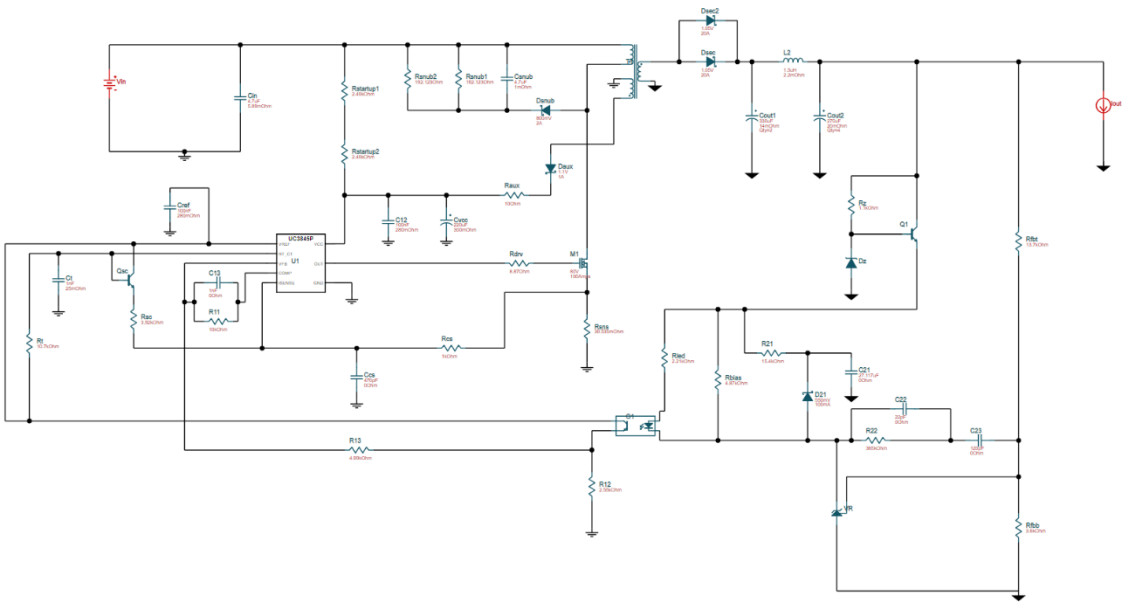

Figure 13. Reference Design of the Flyback Converter with a UC3845 IC

Then, the design is generated in LTSpice for simulations. During the generation of the circuit, the startup resistors and the auxiliary winding are not included, as we will be powering up the

UC3845 with an LM2596 directly from the input. It is tested that the LM2506 can work in the input voltage range of 20-40V, and it can supply the required voltage and current to UC3845.

The schematic of the circuit can be seen in Figure 14.

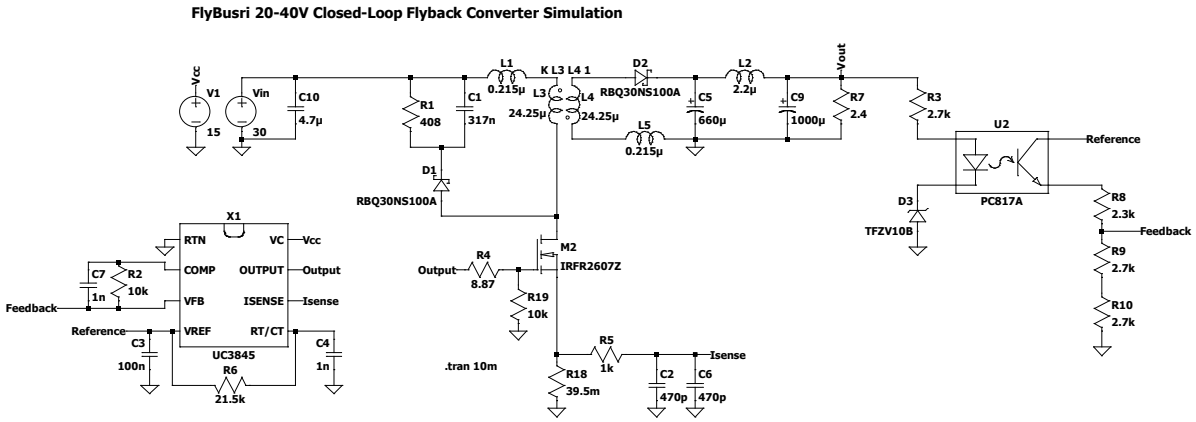

Figure 14. Closed-Loop Circuit Schematic using an UC3845 IC

The simulation consists of the isolated output voltage feedback loop, the RCD clamp, the RC snubber for the switch, output LC filter, and leakage inductances to be able to generate a circuit as close as possible to a real-life application.

The isolated feedback is obtained using an optocoupler. The feedback is generated with a 10V zener diode. The feedback signal generated is sent back to the UC3845 IC.

The RCD clamp is used to decrease the voltage stress on the switching MOSFET. Also, an RC snubber is placed in parallel with the secondary side diode.

The output LC filter helps the circuit to obtain an output which has less ripple on it.

The circuit will be operated both in inputs of 20V and 40V, and the results will be presented.

First, the input voltage is set to $20V$.

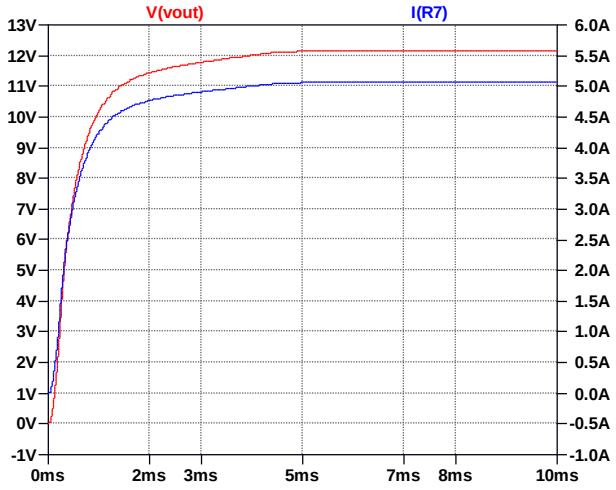

Figure 15. Output Current and Voltage Measurements of the Closed-Loop Circuit for Vin = 20V

Figure 15 represents the output current and voltage of the flyback converter. The response reaches a steady state approximately at 6 milliseconds. It can be seen that the responses include very low ripple at the steady state. The average output current at the steady state is measured as 5.065A and the average output voltage at the steady state is measured as 12.157V. The maximum and minimum values that the output voltage oscillate between are 12.164V and 12.150V respectively. This results in an output voltage regulation of 0.11%. It can be said that the result is in a safe margin as in a real-life application, many non-idealities will be disturbing the circuit, and the results may differ from an ideal scenario. The average input power is 80.695W while the average output power is 61.579W which results in an efficiency of 0.763.

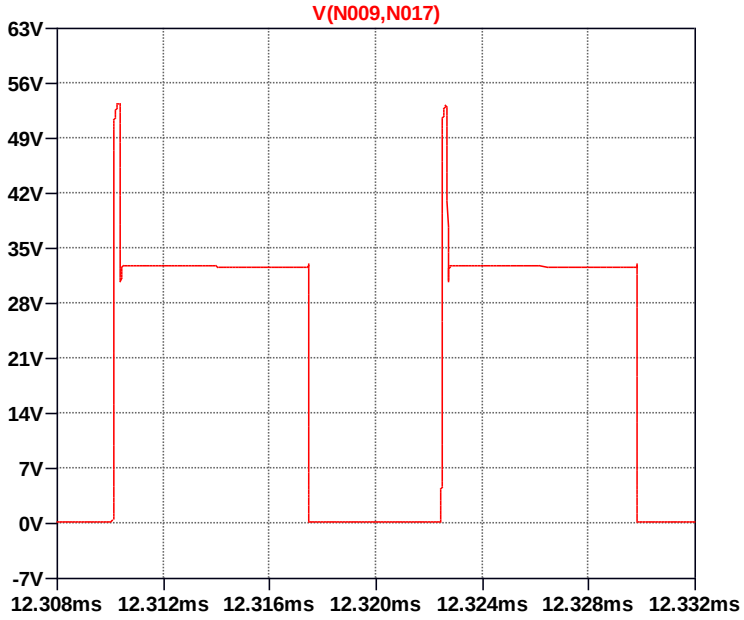

Figure 16. Vds Measurements on the MOSFET for Vin = 20V

The maximum voltage measured on the MOSFET is 53.2V at the steady state. During startup, the voltage on the MOSFET increases to 117V for an instance.

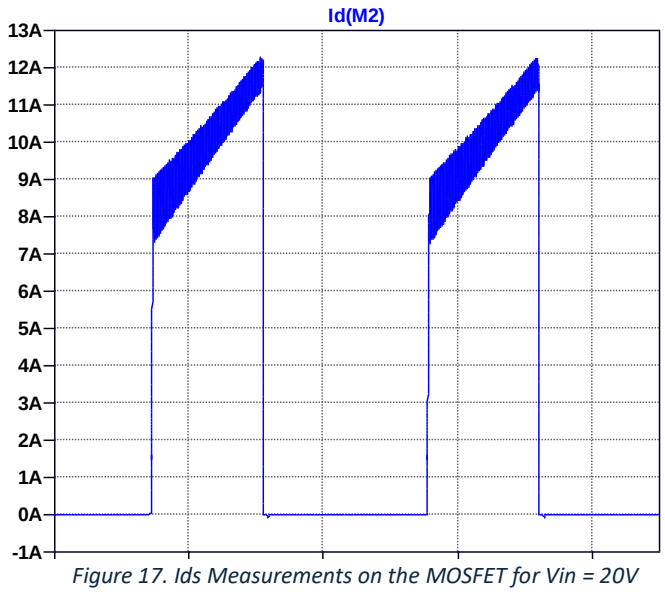

Figure 17. Ids Measurements on the MOSFET for Vin = 20V

The current on the MOSFET increases to 12.28A from 9.012A during the ON period. During startup, the current on the MOSFET increases to 52.8A for an instance. These maximum values of current and voltage on the MOSFET are considered when the components are chosen.

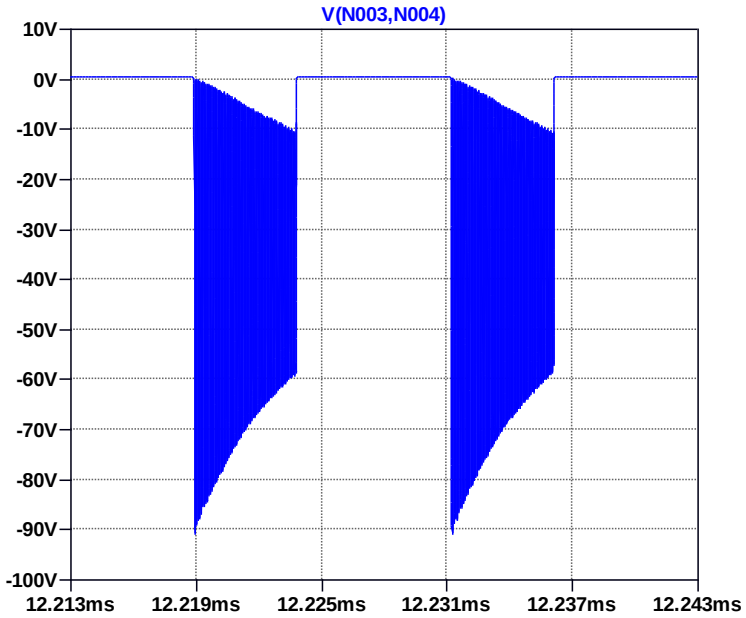

Figure 18. Voltage on the Output Diode for Vin = 20V

The output diode should be able to stand a reverse voltage of 90V. The ringing on it does not induce a power loss as no current passes through it.

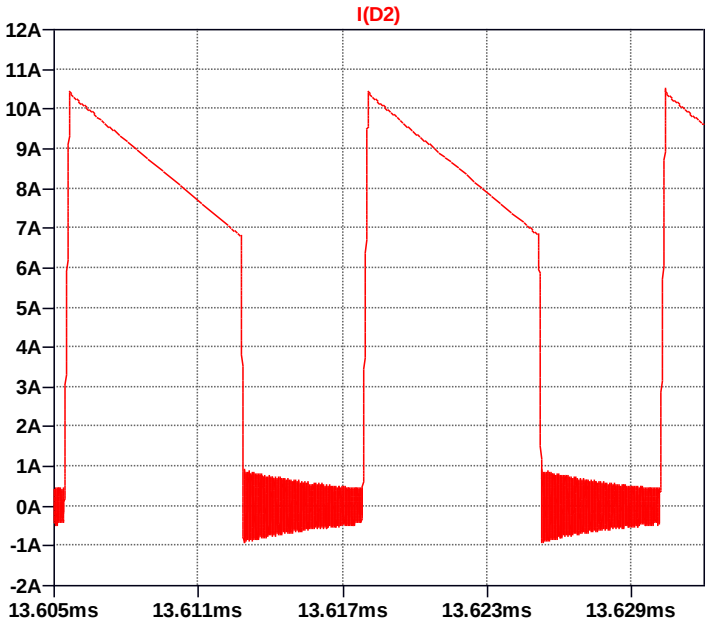

Figure 19. Forward Current on the Output Diode for Vin = 20V

The current on the output diode decreases to 6.81A from 10.39A during a cycle. These maximum values of current and voltage on the output diode are considered when the components are chosen.

Then, the input voltage is set to 40V.

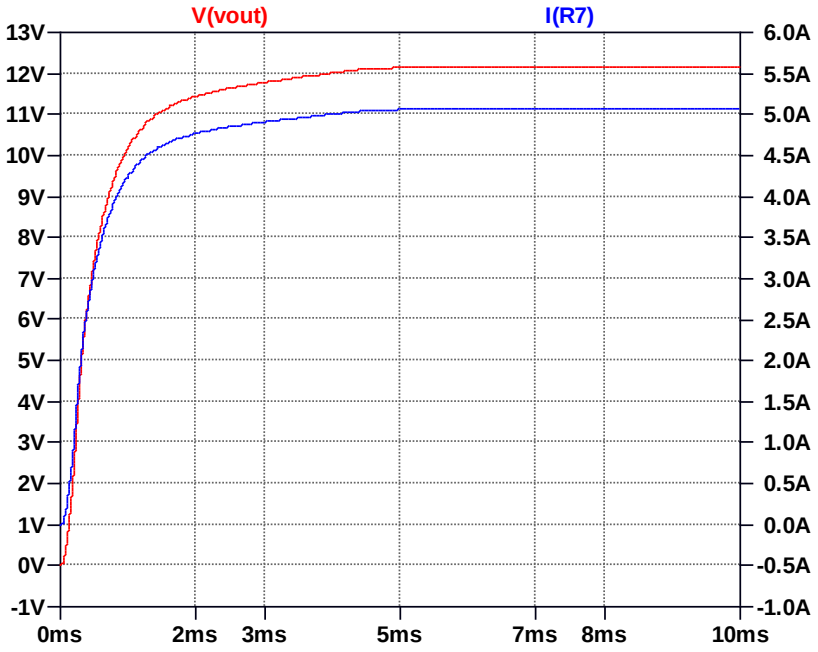

Figure 20. Output Current and Voltage Measurements of the Closed-Loop Circuit for Vin = 40V

Figure 20 represents the output current and voltage of the flyback converter. The response reaches a steady state approximately at 6 milliseconds. It can be seen that the responses include very low ripple at the steady state. The average output current at the steady state is measured as 5.185A and the average output voltage at the steady state is measured as 12.444V. The maximum and minimum values that the output voltage oscillate between are 12.45V and 12.438V respectively. This results in an output voltage regulation of 0.10%. It can be said that the result is in a safe margin as in a real-life application, many non-idealities will be disturbing the circuit, and the results may differ from an ideal scenario. The average input power is 90.603W while the average output power is 64.511W which results in an efficiency of 0.712.

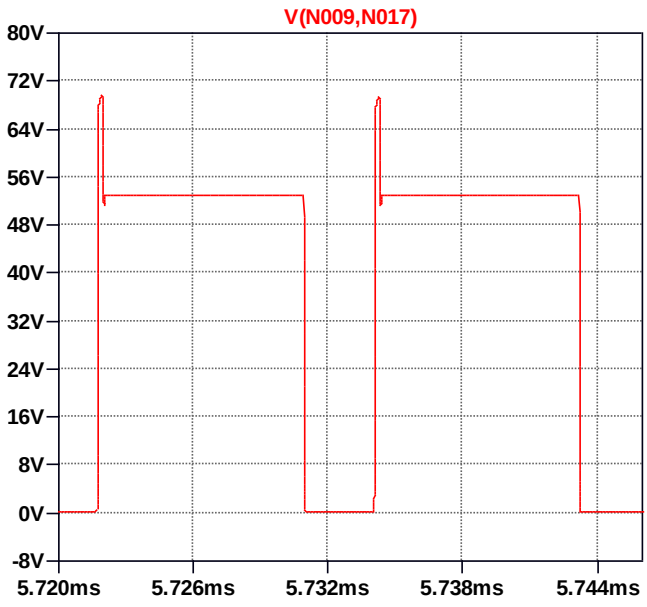

Figure 21. Vds Measurements on the MOSFET for Vin = 40V

The maximum voltage measured on the MOSFET is 69.5V at the steady state. During startup, the voltage on the MOSFET increases to 124V for an instance.

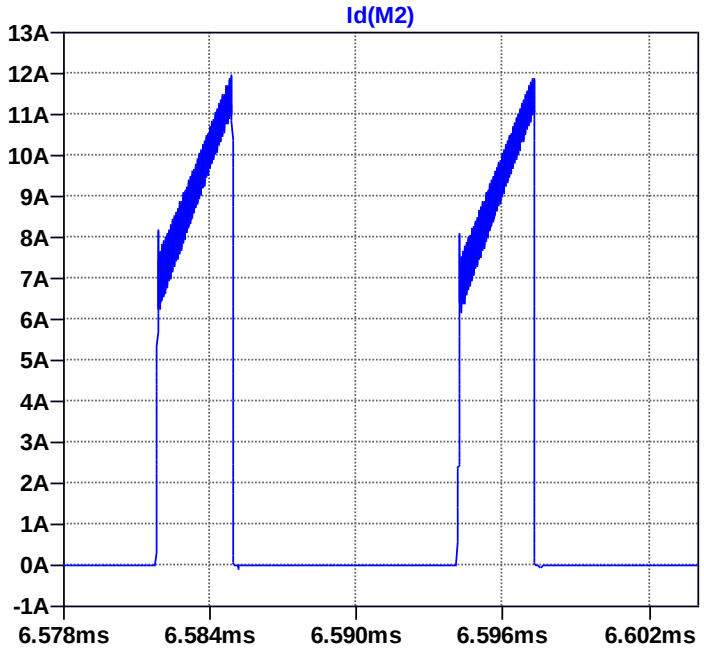

Figure 22. Ids Measurements on the MOSFET for Vin = 40V

The current on the MOSFET increases to 11.95A from 7.637A during the ON period. During startup, the current on the MOSFET increases to 87.5A for an instance. These maximum values of current and voltage on the MOSFET are considered when the components are chosen. Also, the peak one-cycle ratings are considered.

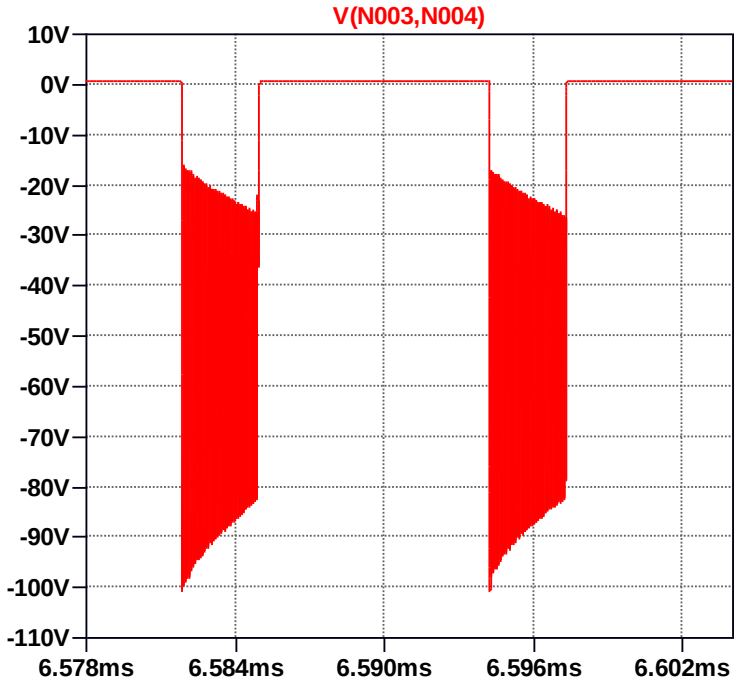

Figure 23. Voltage on the Output Diode for Vin = 40V

The output diode should be able to stand a reverse voltage of 100V. The ringing on it does not induce a power loss as no current passes through it.

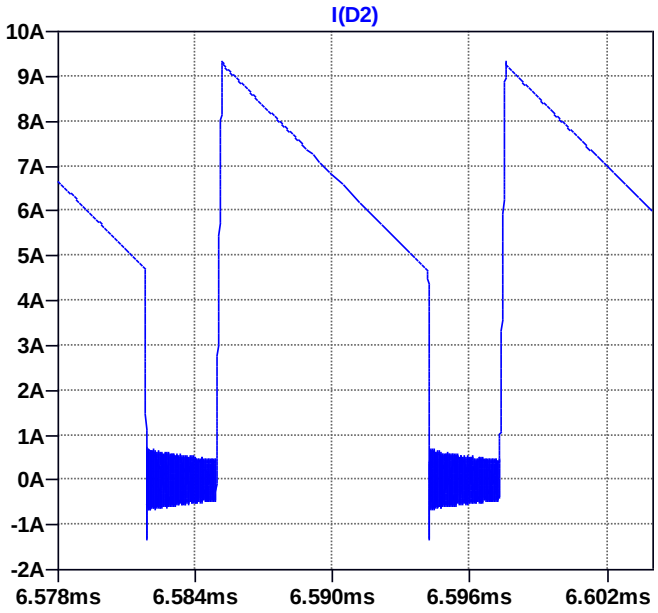

Figure 24. Forward Current on the Output Diode for Vin = 40V

The current on the output diode decreases to 4.76A from 9.41A during a cycle. These maximum values of current and voltage on the output diode are considered when the components are chosen.

Overall, it can be seen that the design can be implemented with a proper choice of the components of the circuit.

Component Selection

The components are mainly picked from the local suppliers such as “ozdisan.com” and “direnc.net”. The most important components for the operation of the converter are the semiconductors such as the switching MOSFET, output diode and clamp diode. The other passive parts and ICs are also found from the mentioned suppliers.

The MOSFET selected is “IRF540NPBF” produced by International Rectifier. It is a 33A 100V N-Channel MOSFET in TO-220AB package with a 44mΩ drain-to-source resistance.

The diode selected for the output and the RCD clamp are same. BD10200CS_S2_00001 is a Schottky diode produced by Panjit in DPAK packaging which can pass through 10A and hold a reverse voltage of 200V. The forward voltage of the diode is equal to 0.9V, which is considered in the design as the additional 1V output that we have considered in the transformer design section.

A 10V zener diode will be used in the feedback generation circuit.

UC3843 will be used as the controller of the circuit. When the datasheet of the controller is inspected, it can be seen that as well as UC3843; UC3844, and UC3845 can be also used as the

properties are exactly same except the operating temperature and duty cycle which does not imply a problem for the project.

The optocoupler used is a PC817 which can be easily found in Turkey.

Transformer Tests

For starters, to verify that the magnetic design is accurate and achievable, transformer windings are manufactured and wound to the core itself. The first design of the transformer is presented below.

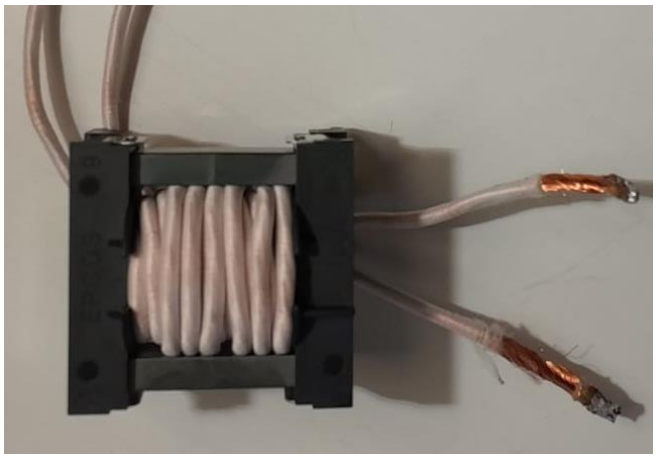

Figure 25. Manufactured Transformer Design

As it is calculated before, the inductance of the primary winding should be approximately 20µH. To achieve this, primary and secondary windings should be 10 turns. After the transformer is manufactured, some tests are conducted to evaluate the parameters of the transformer.

Initially, the primary side of the transformer is connected to the LCR meter, and the inductance and resistance are measured while the secondary is open circuited. Corresponding measurements are given in the figure below.

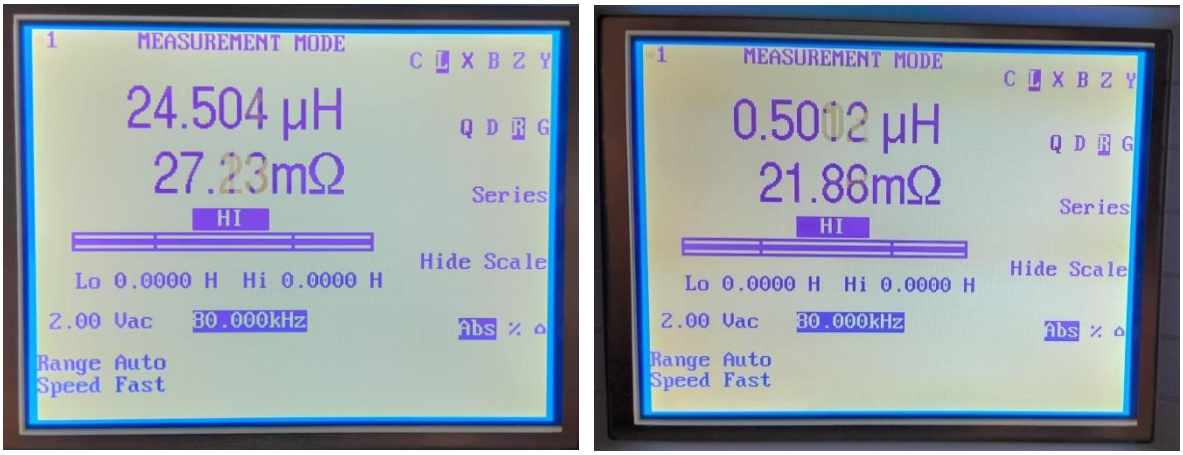

Figure 26. LCR meter measurements: a) secondary side is open circuited, b) secondary side is short circuit.

For the test setup, the equivalent circuit of the transformer is assumed to be as below.

As the turns ratio of the transformer is 1 in this case, leakage for the primary (L1) and the referred secondary leakage inductance (L2) are equal with small possible deviations. For the first test, the LCR meter is connected to the primary side of the transformer while the secondary size is open circuited. Therefore, measured inductance is equal to sum of the leakage inductance and the magnetizing inductance.

$$L_1 + L_m = 24.504\ \mu H$$

For the second test, the secondary side is short circuit. Thus, the measured inductance includes both the primary leakage summed with parallelly connected secondary referred leakage with the magnetizing inductance.

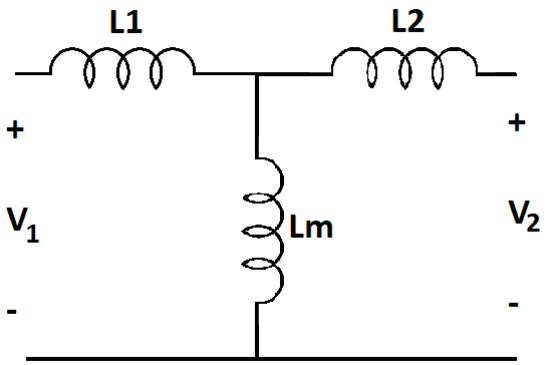

Figure 27. Equivalent Circuit of a Transformer

$$L_1 + L_2//L_m = L_1 + L_1//L_m = 0.5\mu H$$

Using the two equations, leakage inductance and the magnetizing inductance can be calculated. The results show that the magnetizing inductance is significantly higher compared to the leakage inductance. Thus, the second measurement where the secondary side is short circuit, one can assume that the parallel branch does not demand significant current which implies that the measured inductance is approximately equal to twice of the leakage inductance. Lastly, the ratio of the leakage to the magnetizing inductance is calculated as approximately 1% which is reasonable.

$$L_1 \cong 0.2513\ \mu H$$
$$L_m \cong\ 24.2527\ \mu H$$
$$\frac{L_1}{L_m}(\%) = \frac{0.2513}{24.2527} * 100 \cong 1.04\%$$

Final Design

Upon the arrival of the components, the circuit is built on two $10cm\ x\ 10cm$ stripboards, which makes it compact by its size. The final product can be seen in Figure 28.

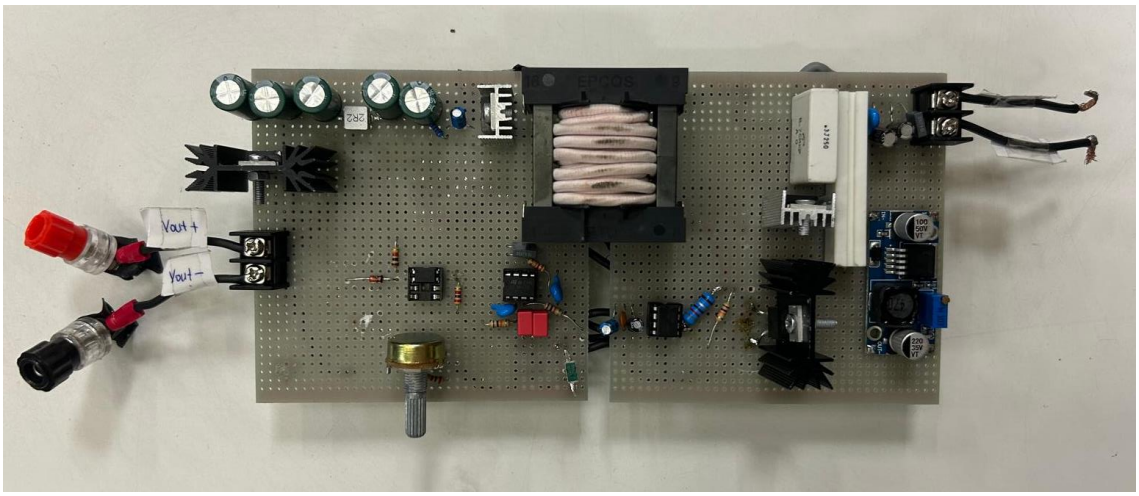

Figure 28. Finalized Product

For easy connection of the DC supply and the load, the pins are generated at the input and output. It can be seen that two sides of the transformer are mounted to two different stripboards. By this, the isolation barrier of the circuit is aimed to be increased. An LM2596 is connected to the input to supply the IC that is used in the circuit with $15V$. From left to right, the IC used are: optocoupler, UC3843 -as the controller-, and IR2106 -as the MOSFET gate driver-.

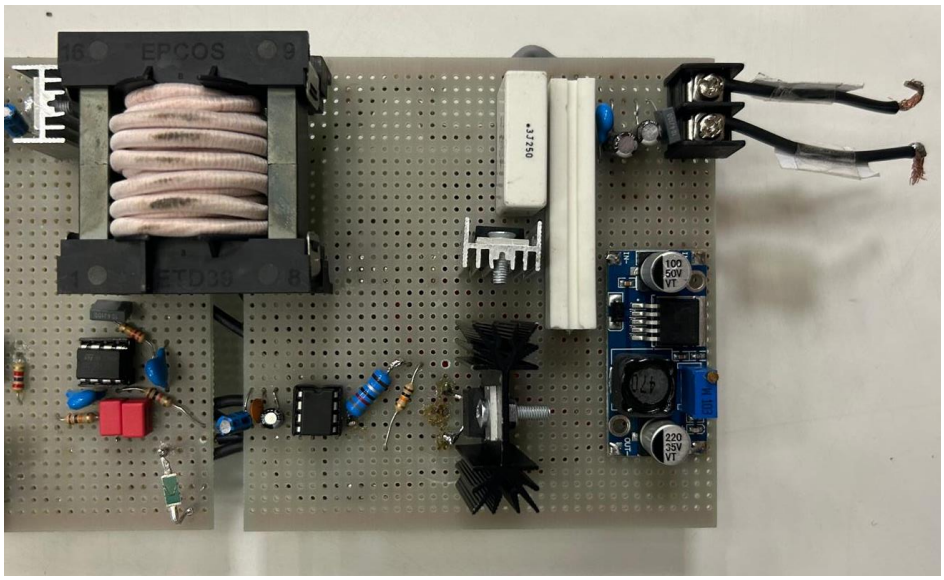

Figure 29. Primary Side of the Flyback Converter

Figure 29 represents the primary side of the flyback converter. The input capacitance is equal to $\sim 500\mu F$. For the snubber, a 390Ω resistor is used in parallel to a $300nF$ film capacitor. The diode used is a DSA60C150PB. The MOSFET used is an IRF540NPBF. In the input

side of the IR2106 gate driver, $1uF$ and $100nF$ capacitors are used. Between the output of the gate driver and the gate of the MOSFET, an $8.82k\Omega$ resistor is used and to discharge the energy in the gate, a $10k\Omega$ resistor is connected between gate and ground. A $50m\Omega$ resistor is used as the sense resistor, and it is connected between source pin of the MOSFET and ground. The controller is the UC3843, which reads the voltage feedback from the output in an isolated way thanks to the optocoupler, and reads the MOSFET current feedback, and then generates a PWM signal in $80kHz$ in the required duty cycle.

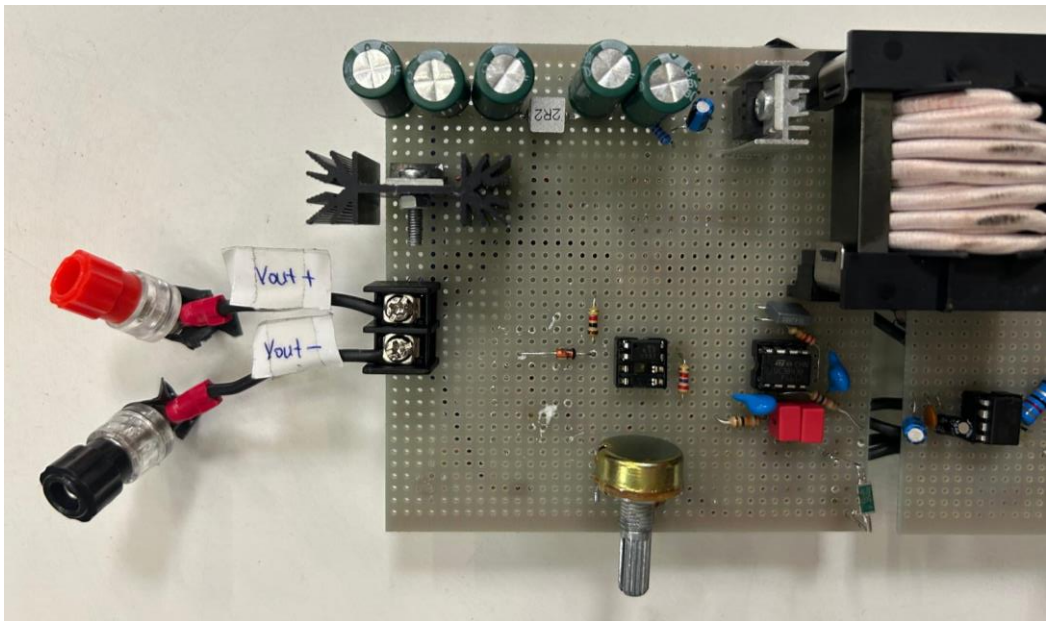

Figure 30. Secondary Side of the Flyback Converter

In the secondary side of the converter, the output diode is selected as same as the diode used in the RCD snubber of the primary side. To decrease the voltage ringing on this diode, an RC snubber circuit is generated via a $2.2k\Omega$ resistor and a $1\mu F$ capacitor. Then, two $330\mu F$ capacitors are placed in order to keep the voltage at the desired level. Then, a low-pass LC filter is designed with a $2.2\mu F$ inductor and three $330uF$ capacitors, which decreases the output voltage ripple. From the output voltage, feedback is generated which can be fine-tuned by the $5k\Omega$ potentiometer, and then sent to the controller in an isolated way via an optocoupler.

After the completion of the product, initial tests are done. it is verified that the load and the line regulations can be done in the given limits, the circuit can operate in the required load, voltage, current, and power conditions. In the next part, the results obtained at the demo day will be represented.

Demo Day Test Results

In the demo day, the 26Ω rheostat is used as the load which is placed at the output of the circuit. DC supply of the laboratory, PSP-405, is used which can supply up to $40V$, and $5A$ at the same time. The results are obtained in two ways. In the first one the input voltage is changed, and the output load is kept constant, and in the second one the input voltage is kept constant, and the output load is changed. In both of the cases the results obtained are same.

Table 2. Test Results

	$V_{in} = 20V$					$V_{in} = 30V$					$V_{in} = 40V$				
$Load$ $(\%, \Omega)$	P_{in} (W)	I_{in} (A)	V_{out} (V)	P_{out} (W)	η $(\%)$	P_{in} (W)	I_{in} (A)	V_{out} (V)	P_{out} (W)	η $(\%)$	P_{in} (W)	I_{in} (A)	V_{out} (V)	P_{out} (W)	η $(\%)$
$25, 9.6$	20,67	1,03	12,36	15,91	76,99	20,37	0,68	12,35	15,89	77,99	21,27	0,53	12,30	15,75	74,07
$50, 4.8$	42,06	2,10	12,22	31,11	73,96	42,25	1,41	12,28	31,41	74,35	43,35	1,08	12,26	31,31	72,22
$75, 3.2$	68,16	3,41	12,18	46,36	68,02	65,14	2,17	12,23	46,74	71,75	66,14	1,65	12,22	46,66	70,54
$100, 2.4$	95,36	4,77	12,12	61,21	64,18	85,17	2,84	12,08	60,80	71,38	90,44	2,26	12,18	61,81	68,34

It can be seen that in all of the cases, the efficiency of the converter varies with respect to the load. The minimum efficiency obtained is 64.18% while the maximum efficiency obtained is 77.99%. The line regulation, and the load regulation specifications of the project are provided. The 3% threshold on all of them when the output voltage is considered as to be $12V$ is equal to $0.36V$. For the load regulation, it can be seen that in all of the input voltage cases, the difference between in the output voltage, when the load is changed from minimum to maximum is less than $0.36V$. Similarly, for the line regulation, under constant load, when the input voltage is varied between $20V$ and $40V$, the change in the output voltage is less than $0.36V$. The project clearly operates and maintains the output voltage within the required limits. Excluding the efficiency limit, the other specifications are confirmed.

An exemplar output voltage and primary side transformer current graphics are represented in Figure 31.

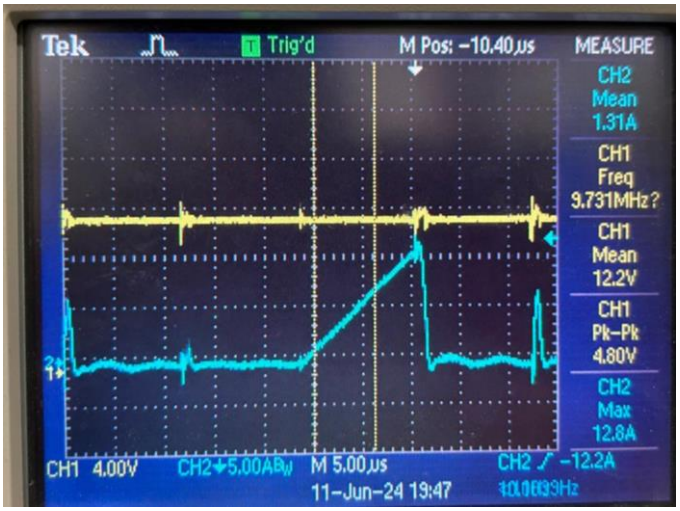

Figure 31. Output Voltage and Transformer Current Measurements

It can be seen that there are minimal peaks in the output voltage and the transformer current occurring at every $12.5\mu s$, which corresponds to the switching frequency of $80kHz$. These are caused by the controller. At every cycle, it opens the MOSFET and checks the voltage on the I_{sense} pin located on the third leg of it. In a case where the energy in magnetizing inductance of the transformer is still enough to power up the load, it directly closes down the MOSFET, so that minimal peaks are observed on the current, and hence the output voltage. When the energy on the magnetizing inductance drops under a value, it charges up the magnetizing inductance, as expected, which is the blue line with a constant slope. It can also be understood that the operating mode of the converter is DCM, which increases the efficiency of the circuit by minimizing the switching losses on the MOSFET. By optimizing the I_{sense} resistance, it is established that the circuit operates in DCM under all load cases.

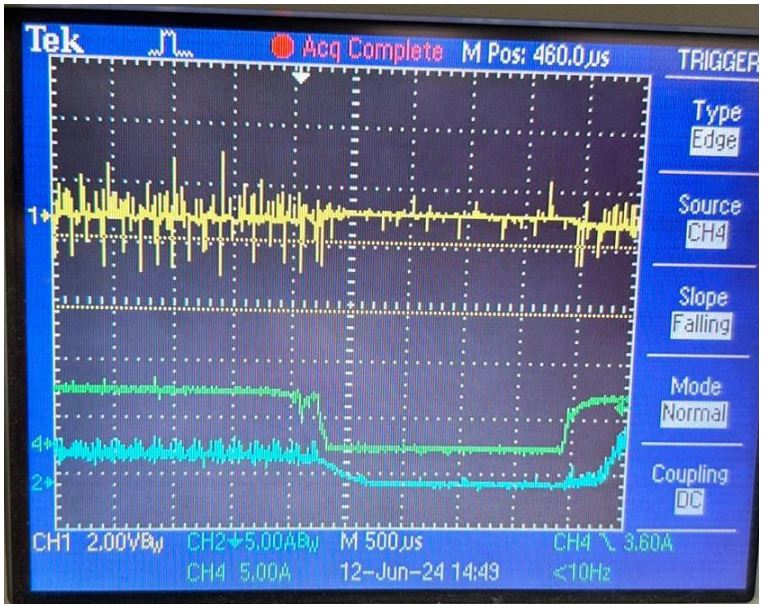

Figure 32. Load Disconnection and Connection Cases

Figure 32 represents a case where under a full load and normal operation, a load disconnection and again a connection occurs. The green line represents the input current and

the output current. It can be seen that when the load is disconnected, the input current directly hits zero, but the output current slowly decays, thanks to the output capacitors. When the load is connected back, the controller can respond to it and the output is again supplied by power, again under full load.

Physical Properties

Thermal Analysis

During the demo day and the previously done experiments on the general design, it can be concluded that all the components can be able to operate under safe operation zone in terms of the temperature ratings. At full load where the current demand is the most, there the elements like MOSFET, diode, etc, which dissipates the heat most, there is no dangerous heating on them. Thus, as the experiments show, the design can be able to operate for reasonably long duration under full load. The most heating element is the MOSFET, and it does not exceed 100 degrees under full load for 5 minutes operation. The figure shows the full load temperature measurements of the final design. Maximum temperature is measured as 76 degrees. Also, figure shows the elements which heats more.

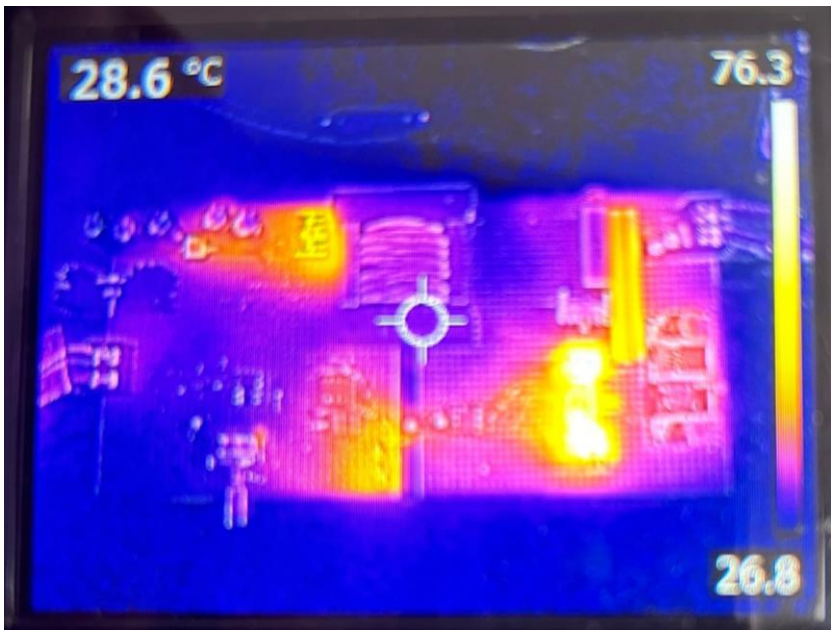

Figure 33. Thermal measurements of the design

The main reason for such high thermal stability is the discontinuous conduction mode. The MOSFET operates at DCM mode which implies that the average current that flows through the MOSFET is considerably less than CCM mode. Thus, the switching element does not heat much so that we can safely operate for reasonably long durations. Thus, overall, design can

stably operate under various conditions including full load condition which does not require and fan for external cooling.

.

Size Analysis

The total area that the circuit is built on is measured from its longest edges and the total volume is calculated accordingly. The measurements are given below.

$$Length = 21 \text{ cm}$$

$$Width = 10cm$$

$$Height = 7 \text{ cm}$$

$$Total\ Volume = 21cm \cdot 10cm \cdot 7cm = 1470\ cm3 = 0.00147\ m3$$

Cost Analysis

For the cost analysis, the prices given in the table are calculated as follows:

$$Total\ Price\ =\ Quantity\ of\ the\ Component\ in\ 1\ Circuit\ \cdot\ 1000$$

Table 3. Cost for 1000 pieces of material

Component	Total Price ($)
B66364A2000X000 Core Clamp	540
B66364W1016T001 Carcass	1450
B66363G0500X187 Core	2840
IRF540NPBF MOSFET	600
IR2106PBF MOSFET Driver	1770
UPC817CG-D04-T Optocoupler	600
LM2596 DC-DC Converter	1090
UC3843N Analog controller	530
Pertinax	1120
DSA60C150PB Schottky Diode	2360
OZDAS0098EL25 Heatsink	640
Others (All resistors, capacitors, etc. expected)	7000

$$Total\ Cost = 20{,}540\ \$\ for\ 1000\ Pieces$$

$$1\ Product = 20.54\ \$$$

Conclusion

This report examines the process of design, implementation, and testing processes of the isolated DC-DC converter project. In the design, considering the final requirements of the project, topology research is finalized, and the flyback converter design is selected and assumed to be good enough for the project requirements. The research and simulation part helped us to understand the overall design broadly and find logical solutions to the predetermined or possible errors. Then, during the implementation step, which was the most educatory and challenging part of the project, different modules are connected to each other to finalize a fully working design where the most unexpected problematic situations are encountered. The members have gained a lot of experience while solving these problems and understood the difference between a simulation environment and a real-life application. Lastly, the circuit was presented on the “Demo Day”. The results of the design were successful and promising.